Combining CT scan and particle imaging techniques: applications in geosciences

Corinne B. Brunelle, Mathieu Des Roches, Louis-Frederic Daigle, Pierre Francus, Bernard Long, Philippe Després

***Abstract*—A small scale physical model of a river and its bed was built to study sediment transport. This model was installed through a CT scanner in order to validate a data acquisition system coupling a CT scan and a particle image velocimetry (PIV) system. The PIV structure is fixed to the scanner, which moves along 2.6 meters rails. This combined system provides high spatial and temporal resolution measurements of bed density and fluid velocity. The data acquisition is time-synchronized and co-located greatly improving our understanding of the dynamics inside the scanned object. The bed topography and porosity as well as the fluid velocity profiles near the bed were successfully derived. These parameters are essential to link hydrodynamic processes over the bed and sediment transport. The methodology holds promising advancements in experimental sedimentology, and could also find interesting applications in other non-medical fields.**

***Index Terms*— CT scan, particle image velocimetry (PIV), physical model, particle-fluid dynamics**

I. Introduction

X-RAY computed tomography (CT) technology has useful applications in geosciences providing density and porosity of non-homogenous materials (Ketcham and Carlson, 2001; Ketcham and Iturrino, 2005; Otani and Obara, 2004). The medical CT scanner is interesting because of its large opening (i.e., 80 cm), allowing a field of view (FOV) up to 65 cm for the reconstructed image. Dynamic systems could also be studied with the CT scan by doing temporally resolved measurements. This paper reports on the use optical imaging techniques to characterize the effect of different flow types on sediment transport. The method consists of coupling a medical CT scanner and a particle image velocimetry (PIV) system. The two datasets are combined to provide an image with density values as well as velocity vectors.

The modeling of sediment transport is one application that would benefit from the proposed methodology since parameterization of shear velocity and sediment density at the boundary layer is essential but otherwise difficult to determine (Sternberg, 1971; Grant and Madsen, 1979). The combined image is interpreted with current knowledge of the sediment dynamics. The specific objectives of this work are to 1) add a high-resolution grid of velocity vectors to the CT scan image and 2) optimize the acquisition parameters to get the best resolution and image quality. Spatial and temporal acquisitions were tested. For spatial measurements, steady flows were used. For temporal measurements, water waves were used considering that the vector field changes rapidly with time. This new perspective would greatly improve the quantification of hydrodynamic properties and sediment transport using experimental work.

C. B. Brunelle, M. Des Roches, L.-F. Daigle, P. Francus and B. Long are with the Multidisciplinary Laboratory of CT Scan for Non-Medical Use, Institut national de la recherche scientifique (INRS), G1K 9A9, Québec, Canada, (corresponding author e-mail: corinne.bourgault-brunelle@ete.inrs.ca). P. Després is with the Université Laval, G1V 0A6, Québec, Canada, (e-mail: philippe.despres@phy.ulaval.ca).

II. Materials and Methods

A movable sand-bed model was built in the Multidisciplinary Laboratory of CT Scan for Non-Medical Use at the Institut National de la Recherche Scientifique (Québec, Canada). A rectangular flume (0.30 m x 0.30 m x 7.0 m) made with 0.025 m thick transparent acrylic material was inserted into a medical X-ray CT scanner (*Siemens*, Somatom Definition AS+ 128) as conducted by Yamada et al. (2013) and Montreuil (2014). The CT scanner moves on 2.6 meters rails along the flume. The water depth in the flume is 0.14 m. The sand bed is composed of quartz (SiO_2), Ottawa sand, with grain median diameter (d_{50}) of 217 µm and uniform density. The bed height is 0.05 m. In addition, as the examination table is static and the gantry moves along the object, the use of large fixed physical models is possible. First, a steady flow is created using a water pump joining the two water tanks placed at each extremity of the flume. A honeycomb diffuser reduces the turbulence at the water inlet. Second, a wavemaker is installed at one extremity to generate waves. A wave absorber made of angular pebbles is placed at the other extremity. The wave period is 1.5 seconds.

A. CT scan measurements

The CT scanner measures attenuation coefficients which are scaled in Hounsfield unit (*HU*). The *HU* values vary from -1024 to +3071 *HU* providing 4096 levels of grey, where air and water values are -1000 and 0, respectively. Images were obtained with a tube current of 600 mAs at a tube voltage of 140 kV. Perfusion mode is used. In this mode, the scan does not move allowing PIV co-located measurements. The collimation is 64 x 0.6 mm providing a set of 64 images every 0.15 seconds (i.e., 6.6 Hz) of the cross-section. In the longitudinal axis, the image is 0.038 m long. The image is reconstructed by a dedicated computer and reconstruction parameters are defined in the *Syngo* software. The convolution

kernel used for the image reconstruction is the B30f which is a relatively soft smoothing filter. The field of view used in the cross-section for the reconstruction is 0.30 m. The isotropic voxel edge length is 0.6 mm. An analogue signal from the CT scan is sent to the PIV for acquisition synchronization.

B. Particle image velocimetry

A LaVision planar particle image velocimetry (PIV) measurement system is mounted on the CT scanner allowing time-synchronized and co-located measurements. To avoid astigmatism effect, a mirror is placed upstream of the scan to reflect the image in the scan zone to the PIV camera located downstream (Fig. 1). The camera is protected from the X-ray by a lead sheet. Image distortion due to optical path or oblique viewing is corrected automatically using a calibration plate. The calibration is a length scale conversion for orthogonal camera viewing. The PIV is set to acquire 2D images of the flow velocity in the longitudinal axis of the flume (sagittal plane). A pulsed laser beam is formed into a light sheet and is fired twice with a short time delay (*dt*). Both illuminations are recorded by one double-frame high resolution CCD camera. The recorded pair of images is divided into small interrogation windows of 32 x 32 pixels. The resulting vector field grid resolution is 1 mm and the field of view is 0.35 m x 0.29 m. The *dt* is adjusted according to the measured velocities to make sure that the movement of a particle is smaller than a quarter of the interrogation window size. The *dt* value is 6 ms for steady flow and 11 ms for waves. Increasing the *dt* increase the detection of high velocity but neglect the slow movements. It appeared that the *dt* was unnecessarily short for steady flow and was increased for waves, for which the *dt* was fast enough. During the time interval *dt*, between the laser shots, the particles of each interrogation window have moved by a displacement *ds*. The velocity is then simply given by the ratio *ds*/*dt*. The calculation of the particle displacement *ds* is done by fast FFT-based cross-correlation of two corresponding interrogation windows. Only vectors calculated with a great correlation are conserved. The interrogation window overlap is 75 %, which has the effect of smoothing the velocity vector field. The PIV system samples at 6.66 Hz during 3 seconds and starts at the same time as the CT scan measurements. This way, there is one PIV grid of vector for each CT scan image. There is approximately one velocity vector for two CT scan pixels.

C. Data post-treatment

The *HU* values can directly be interpreted as a function of density in this study because the sand used is 99.5% pure silica (i.e., uniform) and a voxel can only contain water and sand. Otherwise, the regression used to convert *HU* values into density would vary as a function of the atomic numbers (Boespflug et al. 1994). The artefacts in the water column mostly affect the side of the image in the cross-section. Thus, only pixels in the center of the flume are interpreted. In the longitudinal axis, this area corresponds to the PIV plane of the flume. However, *HU* values in the ripple region itself need to be interpreted with care because streaks can appear near the bed. The interface of water and sand is first determined by thresholding. The sand density (ρ_s) is determined by equation (1), where the measured *HU* value (HU_m) is compared to *HU* value of water (HU_w) and of pure quartz (HU_q) using the density of pure quartz (ρ_q).

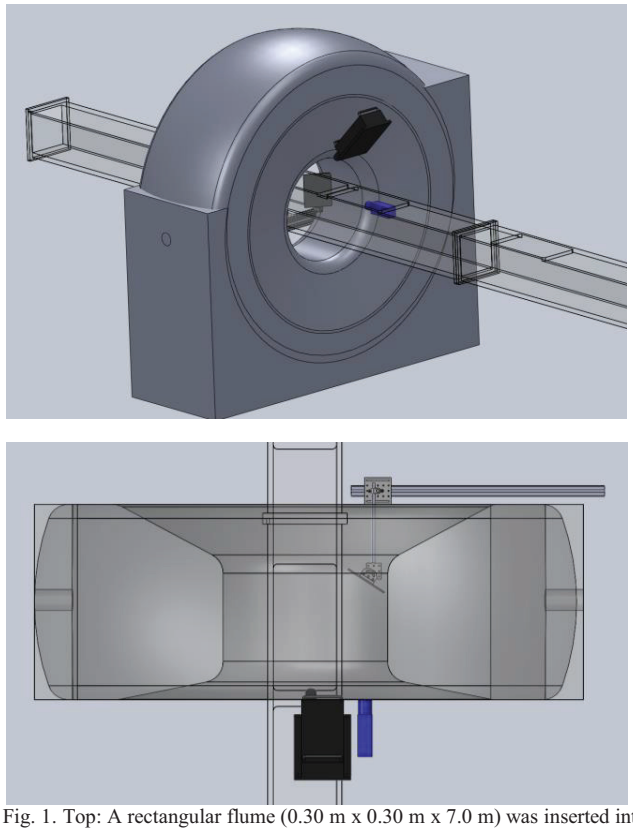

Fig. 1. Top: A rectangular flume (0.30 m x 0.30 m x 7.0 m) was inserted into a medical X-ray CT scanner (Siemens, Somatom Definition AS+ 128). The PIV system is fixed to the CT scanner. Bottom: The laser (black) of the PIV system shoots in the CT scan measurement zone, the light is reflected to the mirror (on the support) and back projected to the camera (blue).

$$\rho_s = \left(\frac{HU_m - HU_{H2O}}{HU_q - HU_{H2O}}\right)\rho_q \qquad (1)$$

The porosity (n) is defined as:

$$\rho_s = (1 - \mathrm{n})\rho_q \qquad (2)$$

The porosity of well-sorted sand is approximately 0.4, meaning that 0.6 (i.e., 1-0.4) multiplied by the pure quartz density (2.64 g/cm^3) is equal to the sand bed density (1.6 g/cm^3). The images of the CT scanner and the PIV are superposed using a reference point with a known position in the two coordinate systems, which is located on a PIV calibration plate. This plate is also scanned with the CT scanner. Only instantaneous measurements are shown in the results section (i.e., snapshots).

III. Results and Discussion

Co-located and time synchronized images of fluid motion are taken over a ripple. The experimental setup is used to test two types of acquisition sequences. First, the PIV and the CT scanner, which are fixed together, move at different locations in a short period of time to describe the hydrodynamics of a steady flow in space (section A). Second, the PIV system and the CT scanner are located at a fixed point making fast temporal measurements of wave motion (section B).

A. Spatial analysis of a steady flow

The PIV and the CT scan measure the flow properties in front of a ripple (Fig. 2a). Then, the scanner is moved after 30 seconds on the top of the ripple for another 3 seconds of measurements (Fig. 2b). The scan is moved again after 30 seconds behind the ripple (Fig. 2c). The ripple moves in the current direction. The results show that the hydrodynamics of a steady flow over a ripple are observed with high spatial resolution. The velocity profiles near the bed determine the bottom shear stress (τ_b). This parameter is important because it is related to the force per unit area acting on the sand bed. The sediment transport is a function of that parameter as well as the grain size and the porosity of the bed (Van Rijn, 1984). The reference bed porosity value 0.4 gives a sand bed density (ρ_s) of 1.6 g/cm^3, which is similar to measurements. The sand-water interface (dashed black line) is delimitated by using a threshold *HU* value (i.e., 1400). This way, it is possible to calculate the ripple displacement by doing repetitive scans. Consequently, the bedload transport of sediments can be calculated. The front face of the ripple (i.e., the stoss face) is the divergence zone resulting in erosion. The so-called lee face is the convergence zone on the trailing edge of the ripple, where accretion results in ripple migration.

B. Temporal periodicity of wave motion

The PIV and the CT scan do not move and they measure only in the ripple trough (Fig. 3). The images show the hydrodynamic features of a wave passage in that area. The ripple trough is a zone of interest for sediment transport because sand re-suspension by eddies are expected there. The vector orientation and length are coherent with typical wave induced movements (i.e., orbital). The current is oriented in the wave propagation direction under the wave crest (Fig. 3a). Then, the current is oriented downward during the wave trough approach (Fig. 3b) and finally totally reverses, little oriented upward, before the passage of the second wave (Fig. 3c).

It would be expected to find higher sediment concentration just after the wave passage. Further analyses of CT artefacts are needed to better quantify the suspended matter concentration in that region. The problem is the change in geometry of the experimental setup (e.g., the wave passage or ripple formation) which changes the absolute *HU* values within the image. However, the technique shows the potential to characterize rapid flow variations and bed deformation with time.

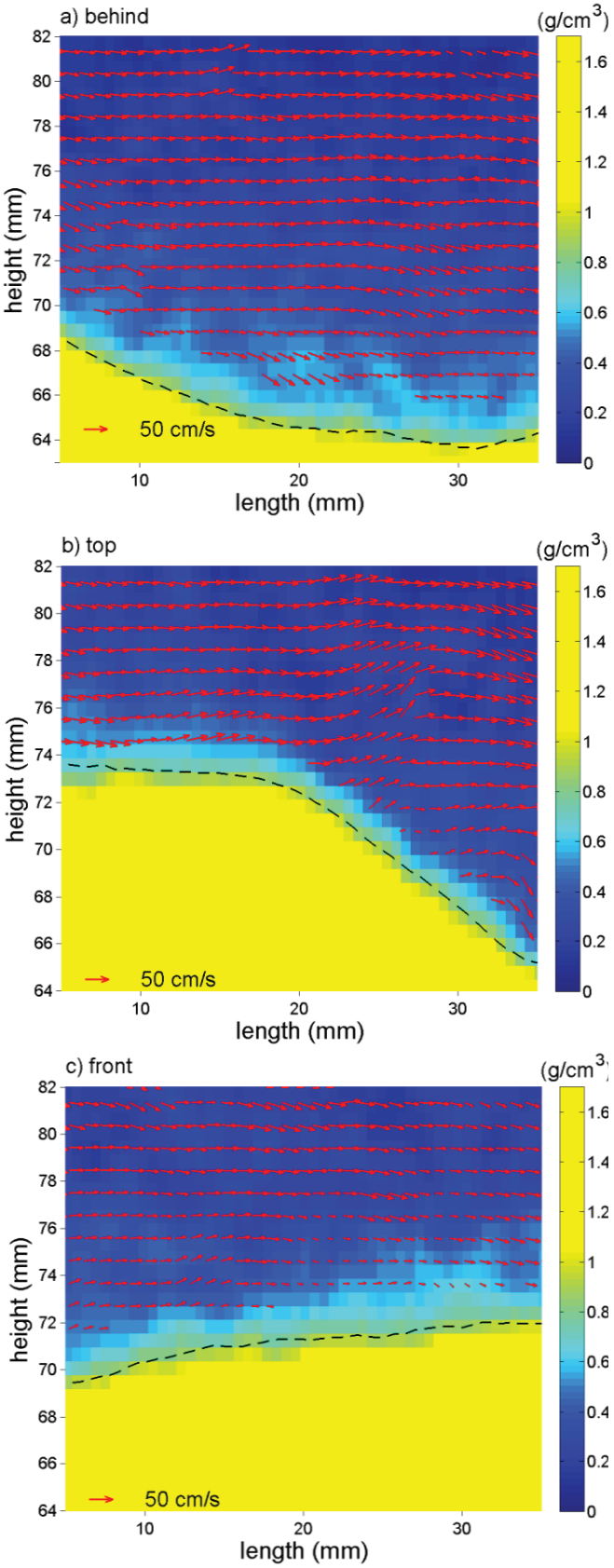

Fig. 2. Sand ripple and steady flow: instantaneous sediment density is measured with the CT scanner (colored background) combined with fluid velocity vectors measured using the PIV (red vectors). The hydrodynamics of a steady flow is illustrated a) behind, b) on the top and c) in the front of the ripple (yellow). The time lap between two images is approximately 30 seconds.

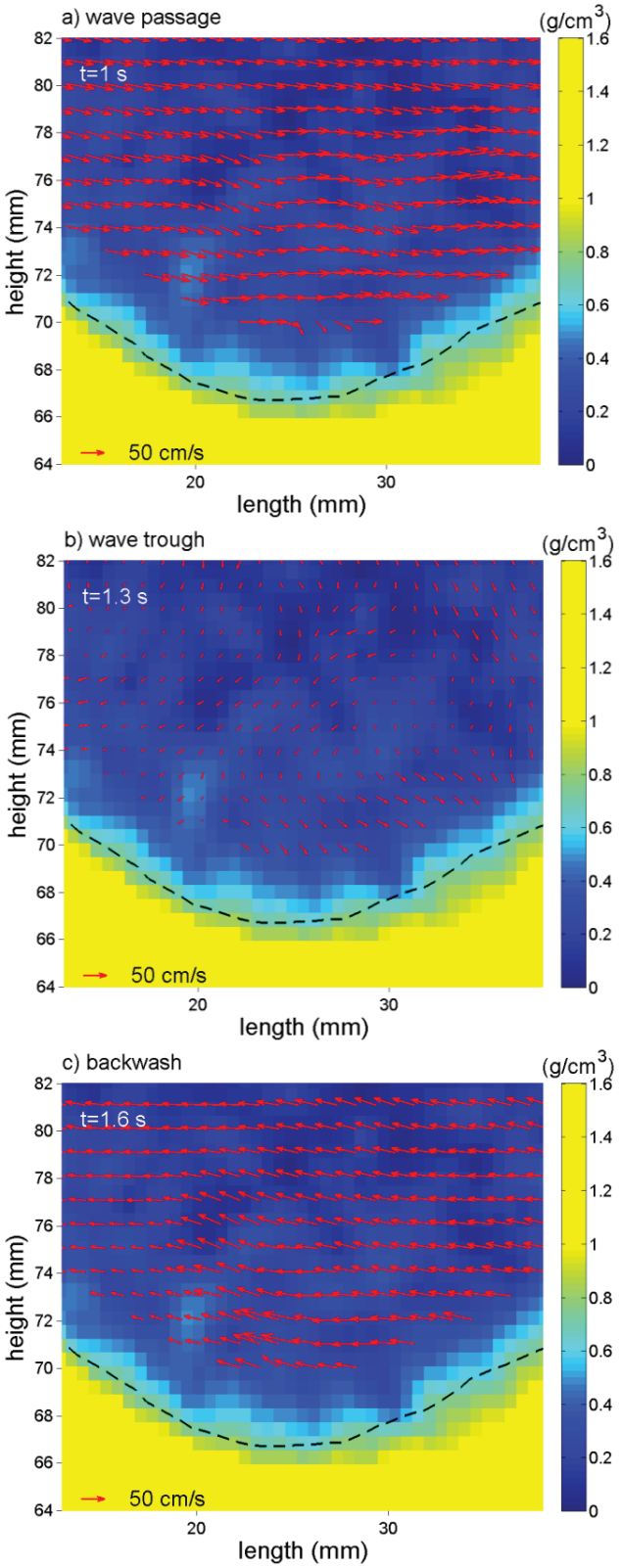

Fig. 3. Ripple trough and wave current: instantaneous sediment density measured with the CT scanner (colored background) combined with fluid velocity vectors measured using the PIV (red vectors). The hydrodynamics induced by waves in the ripple trough (yellow) is illustrated for a) the wave passage, b) the wave trough and c) the backwash occurring before the wave passage (i.e., approaching wave). The time lap between two images is approximately 0.3 s and the wave period is 1.5 s.

IV. Conclusion

The PIV system was successfully synchronized with the CT scanner. This adds velocity vectors to the image of density that could ultimately give the transport rate of sediments. This is fundamental information to understand the physics of particle-fluid dynamics and improve the modeling of the underlying processes, and was never achieved before. Still, we made several observations to be taken into account to improve further experiments. The stability of the experimental setup is fundamental and the image appears to be really sensitive to that factor. The acquisition restriction mostly comes from tube thermal loading. The noise in the water pixels greatly affects the accuracy of suspended particle concentration detection. By optimizing the tube voltage and current as well as the beam collimation, the pause between the scans and the noise in the image could be reduced. For the X-ray image artefacts, further work will be conducted to better described the effects of the geometry setup on the reconstructed image as well as test different reconstruction algorithms. The beam hardening artifacts are also a challenge that needs to be addressed considering that no correction is applied for sand. Overall, the experiment showed interesting results that could have many applications in different non-medical research field providing a fast temporal acquisition and high spatial resolution data.

Acknowledgment

The authors want to thank the Canada Foundation for Innovation for their financial contribution, *Siemens* for their support and the Government of Québec (Ministère des Transports & Ministère de la Sécurité publique) for the student scholarships.

References

Boespflug, X., N. Ross, B. Long, and J. F. Dumais. 1994. "Tomodensitométrie Axiale: Relation Entre L'intensité Tomographique et La Densité de La Matière." Canadian Journal of Earth Sciences 31 (2): 426–34.

Grant, William D., and Ole Secher Madsen. 1979. "Combined Wave and Current Interaction with a Rough Bottom." Journal of Geophysical Research: Oceans (1978–2012) 84 (C4): 1797–1808.

Ketcham, Richard A., and William D. Carlson. 2001. "Acquisition, Optimization and Interpretation of X-Ray Computed Tomographic Imagery: Applications to the Geosciences." Computers & Geosciences 27 (4): 381–400.

Ketcham, Richard A., and Gerardo J. Iturrino. 2005. "Nondestructive High-Resolution Visualization and Measurement of Anisotropic Effective Porosity in Complex Lithologies Using High-Resolution X-Ray Computed Tomography." Journal of Hydrology 302 (1): 92–106.

Otani, Jun, and Yuzo Obara. 2004. Xray CT for Geomaterials: Soils, Concrete, Rocks International Workshop on Xray CT for Geomaterials, Kumamoto, Japan. CRC Press.

Montreuil, S. 2014. "Définition des paramètres sédimentologiques mesurés au scanographe densitométrique et estimation de la contrainte de cisaillement sur une ride sableuse. " Thèse. Québec, Université du Québec, Institut national de la recherche scientifique, Doctorat en sciences de la terre, 340 p.

Sternberg, Richard W. 1971. "Measurements of Incipient Motion of Sediment Particles in the Marine Environment." Marine Geology 10 (2): 113–19.

Van Rijn, L. C. 1984. "Sediment Transport, Part I: Bed Load Transport. " Journal of Hydraulic Engineering 110 (10): 1431–56.

Yamada, Fumihiko, Ryuta Tateyama, Gozo Tsujimoto, Seiya Suenaga, Bernard Long, and Constant Pilote. 2013. "Dynamic Monitoring of Physical Models Beach Morphodynamics and Sediment Transport Using X-Ray CT Scanning Technique." Journal of Coastal Resarch, 1617–22.